

Improved Generalized Automorphism Belief Propagation Decoding

Jonathan Mandelbaum, Sisi Miao, Nils Albert Schwendemann, Holger Jäkel, and Laurent Schmalen
Communications Engineering Lab, Karlsruhe Institute of Technology (KIT), 76131 Karlsruhe, Germany

jonathan.mandelbaum@kit.edu

Abstract—With the increasing demands on future wireless systems, new design objectives become eminent. Low-density parity-check codes together with belief propagation (BP) decoding have outstanding performance for large block lengths. Yet, for future wireless systems, good decoding performance for short block lengths is mandatory, a regime in which BP decoding typically shows a significant gap to maximum likelihood decoding. Automorphism ensemble decoding (AED) is known to reduce this gap effectively and, in addition, enables an easy trade-off between latency, throughput, and complexity. Recently, generalized AED (GAED) was proposed to increase the set of feasible automorphisms suitable for ensemble decoding. By construction, GAED requires a preprocessing step within its constituent paths that results in information loss and potentially limits the gains of GAED. In this work, we show that the preprocessing step can be merged with the Tanner graph of BP decoding, thereby improving the performance of the constituent paths. Finally, we show that the improvement of the individual paths also enhances the overall performance of the ensemble.

Index Terms—generalized automorphism groups; generalized automorphism ensemble decoding; short block lengths codes; 6G

I. INTRODUCTION

With the ongoing rollout of 5G, research activities shift their focus onto the analysis of enabling technologies for the next-generation 6G wireless systems [1]. The rising demand for flexibility to adapt to different use cases, e.g., ultra reliable and low latency communications (URLLC), also impacts the channel coding scheme. This shift yields new expected design objectives, e.g., low latency and reduced decoding complexity [2], [3]. Thereby, unified coding is a candidate for becoming an enabling technology for a future 6G channel coding scheme [2]. Herein, unified coding refers to a single code family that performs well in the different specified scenarios by, e.g., employing different decoders [2]. In particular, low-density parity-check (LDPC) codes, first introduced by Gallager [4] together with a low-complexity iterative decoding scheme often denoted as belief propagation (BP) decoding, have outstanding decoding performance for large block lengths [5]. However, for future use cases, e.g., URLLC scenarios, short block length codes are unavoidable, a regime in which the BP decoding performance of LDPC shows a significant gap to the performance of maximum likelihood (ML) decoding. Yet, BP

decoding provides benefits, e.g., low latency and simple hardware implementation. Therefore, one step towards a potential unified coding scheme is to improve the performance of BP based decoding schemes in the short block length regime.

Ensemble decoding schemes such as, e.g., multiple bases belief propagation (MBBP) [6], [7], automorphism ensemble decoding (AED) [8], [9], generalized AED (GAED) [10], and endomorphism ensemble decoding (EED) [11], can enhance the performance of BP decoding for short block length codes and provide flexibility in the trade-off of complexity, throughput, and latency. They exploit the fact that the successful decoding of the received word at the output of a binary-input memoryless symmetric output channel (BMS-C) with BP decoding is determined by the realization of the noise, rather than the respective codeword [5, Lemma 4.90]. Automorphism-based ensemble decoding algorithms, i.e., AED and GAED, perform parallel decoding operations in parallel paths each relying on an alternative noise representation.¹

The most prominent definition of the automorphism group of channel codes stems from [12] where the authors define the automorphism group of a binary code to consist of all permutations that are self-mappings of the code. Recently, in [10], we proposed a more general definition of the automorphism group defining it as the set of all linear bijective self-mappings. Furthermore, we introduced the concept of GAED demonstrating that generalized automorphisms can be used for decoding [10]. Hereby, the paths of a GAED require a preprocessing step which results in an information loss and reduces the decoding gains achieved by the ensemble scheme.

In this work, we improve GAED by reducing the losses due to the preprocessing. To this end, we first demonstrate that the preprocessing required for GAED can be merged with the Tanner graph of the code, resulting in a larger Tanner graph which is then used for decoding. We name this algorithm improved GAED (iGAED). Herein, “improved” refers to two possible benefits achieved by this construction: On the one hand, decoding performance with respect to error rate is improved by avoiding information loss during preprocessing, particularly in the high SNR regime. On the other hand, implicitly realizing mapping (2) within the Tanner graph may be advantageous for hardware implementation.

This work has received funding from the German Federal Ministry of Education and Research (BMBF) within the project Open6GHub (grant agreement 16KISK010) and the European Research Council (ERC) under the European Union’s Horizon 2020 research and innovation programme (grant agreement No. 101001899).

¹In addition, AED and GAED allow for different decoding algorithms in their respective paths, e.g., using BP decoding based on different parity check matrices (PCMs) and, hence, incorporating ideas of MBBP [6]. Note that in each path, a PCM with redundant rows may be used.

II. PRELIMINARIES

A. Linear Block Codes

A binary linear block code $\mathcal{C}(n, k)$ consists of 2^k distinct vectors that form a k -dimensional subspace of the vector space \mathbb{F}_2^n , where the parameters $n \in \mathbb{N}$ and $k \in \mathbb{N}$ denote block length and information length, respectively. For simplicity, we omit the parameters (n, k) when obvious from the context. Note that vectors are column vectors. Linear block codes can be expressed as the null space of their parity-check matrix (PCM) $\mathbf{H} \in \mathbb{F}_2^{m \times n}$ [12], i.e.,

$$\mathcal{C}(n, k) = \{\mathbf{x} \in \mathbb{F}_2^n : \mathbf{H}\mathbf{x} = \mathbf{0}\} = \text{Null}(\mathbf{H}).$$

BP decoding is an iterative message passing algorithm on the Tanner graph of the code [5]. A Tanner graph is a bipartite graph with two disjoint sets of vertices: the variable nodes (VNs) \mathfrak{V} corresponding to the code bits x_i , and, thus, the columns of \mathbf{H} , and the check nodes (CNs) \mathfrak{C} corresponding to the parity checks and, thus, to rows of \mathbf{H} . A VN $v_i \in \mathfrak{V}$ is connected to a CN $c_j \in \mathfrak{C}$ if the corresponding entry $H_{j,i} = 1$. Messages are iteratively propagated along the edges and updated in the nodes of the graph [5]. A linear code can be expressed by different Tanner graphs. The performance of BP decoding dominantly depends on the degrees of the nodes and the short cycles within the Tanner graph and, hence, the performance typically differs when decoding on the different Tanner graph representations of a code [5].

B. Automorphism Group

In [12], the automorphism group of a binary linear code is defined as

$$\text{Aut}(\mathcal{C}) := \{\pi : \mathcal{C} \rightarrow \mathcal{C}, \mathbf{x} \mapsto \pi(\mathbf{x}) : \pi \in S_n\},$$

with $\pi(\mathbf{x}) = (x_{\pi(1)}, \dots, x_{\pi(n)})^T$ and S_n being the symmetric group [12]. Therefore, it consists of all index permutations that map codewords onto codewords. In [10], a different view on the automorphism group of codes is introduced, using the more general notion prominent in linear algebra. To this end, the generalized automorphism group of a binary linear code \mathcal{C} is defined as

$$\text{GAut}(\mathcal{C}) := \{\tau : \mathcal{C} \rightarrow \mathcal{C} : \tau \text{ linear, } \tau \text{ bijective}\}.$$

The (permutation) automorphism group $\text{Aut}(\mathcal{C})$ is a subgroup of the generalized automorphism group $\text{GAut}(\mathcal{C})$ [10]. Furthermore, note that a linear mapping $\tau : \mathcal{C} \rightarrow \mathcal{C}$ can be expressed by a transformation matrix $\mathbf{T} \in \mathbb{F}_2^{n \times n}$, i.e.,

$$\mathbf{x}_\tau := \tau(\mathbf{x}) = \mathbf{T}\mathbf{x} \in \mathcal{C}. \quad (1)$$

Since $\tau \in \text{GAut}(\mathcal{C})$ is only assumed to be bijective on \mathcal{C} and not on \mathbb{F}_2^n , its transformation matrix \mathbf{T} is not necessarily non-singular. However, for the sake of simplicity, we only consider cases in which \mathbf{T}^{-1} exists, as in [10].

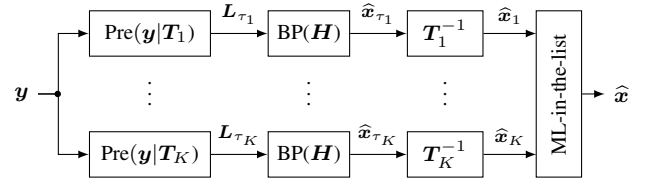


Fig. 1. Block diagram of GAED introduced by [10] in which K different automorphisms with transformation matrices \mathbf{T}_ℓ are used. We assume that each path performs BP decoding based on the PCM \mathbf{H} .

C. Generalized Automorphism Ensemble Decoding

AED as a generalization of MBBP decoding was first introduced in [8] and further generalized to GAED in [10]. Figure 1 depicts a block diagram of GAED based on BP decoding which we will briefly recapitulate.

Consider the transmission of a binary codeword $\mathbf{x} \in \mathcal{C} \subset \mathbb{F}_2^n$ over a BMSC. At the channel output, $\mathbf{y} \in \mathcal{Y}^n$ is observed (with \mathcal{Y} being the output alphabet) and then mapped onto the bit-wise LLR vector $\mathbf{L} := (L(y_j|x_j))_{j=1}^n \in \mathbb{R}^n$. Then, if $\mathbf{T}_1, \dots, \mathbf{T}_K$ are the non-singular transformation matrices of K generalized automorphisms used for GAED, the ensemble decoding consists of K parallel paths each including a preprocessing block, a BP decoding block, and an inverse mapping block.

In path $\ell \in \{1, \dots, K\}$, the j th element, $j \in \{1, \dots, n\}$, of bit-wise LLR vector \mathbf{L} is preprocessed according to [10]:

$$(\mathbf{L}_{\tau_\ell})_j := (\text{Pre}(\mathbf{y}|\mathbf{T}_\ell))_j := \bigoplus_{\substack{i=1, \\ T_{\ell,j,i}=1}}^n L(y_i|x_i), \quad (2)$$

with the box-plus operator \boxplus introduced in [13] to imitate the \mathbb{F}_2 summation in (1) in the LLR domain. Note that variables with subscript τ , e.g., \mathbf{L}_{τ_ℓ} , denote values after preprocessing as introduced in (1). If \mathbf{T}_ℓ is the transformation matrix of a permutation automorphism $\tau_\ell \in \text{Aut}(\mathcal{C})$ then the preprocessing corresponds to the permutation of LLRs known from AED [10].

Next, the preprocessed LLR vector \mathbf{L}_{τ_ℓ} is decoded by a BP decoder, resulting in an estimate $\hat{\mathbf{x}}_{\tau_\ell}$. If BP decoding converges to a codeword, i.e., if $\hat{\mathbf{x}}_{\tau_\ell} \in \mathcal{C}$, then $\hat{\mathbf{x}}_{\tau_\ell}$ constitutes an estimate of the codeword after the preprocessing, i.e., $\hat{\mathbf{x}}_{\tau_\ell} = \mathbf{T}_\ell \mathbf{x}_\ell$. Hence, to compensate for the effect of preprocessing, $\hat{\mathbf{x}}_{\tau_\ell}$ has to be post-processed with the inverse automorphism \mathbf{T}_ℓ^{-1} to obtain an estimate of the originally transmitted codeword, i.e., $\hat{\mathbf{x}}_\ell = \mathbf{T}_\ell^{-1} \hat{\mathbf{x}}_{\tau_\ell}$.

Finally, GAED collects the K estimates of all paths in an *ML-in-the-list* block that outputs the final estimate $\hat{\mathbf{x}}$ according to the *ML-in-the-list* rule described in [8].

In [10], the impact of the *weight over permutation*

$$\Delta(\mathbf{T}) = \sum_{i,j} T_{i,j} - n$$

is analyzed. It is demonstrated that larger weight over permutations leads to an increasing information loss due to the preprocessing that results in a degradation of the performance of that path. Yet, as shown in [10], GAED still can exploit the additional diversity of the degraded parallel paths to improve

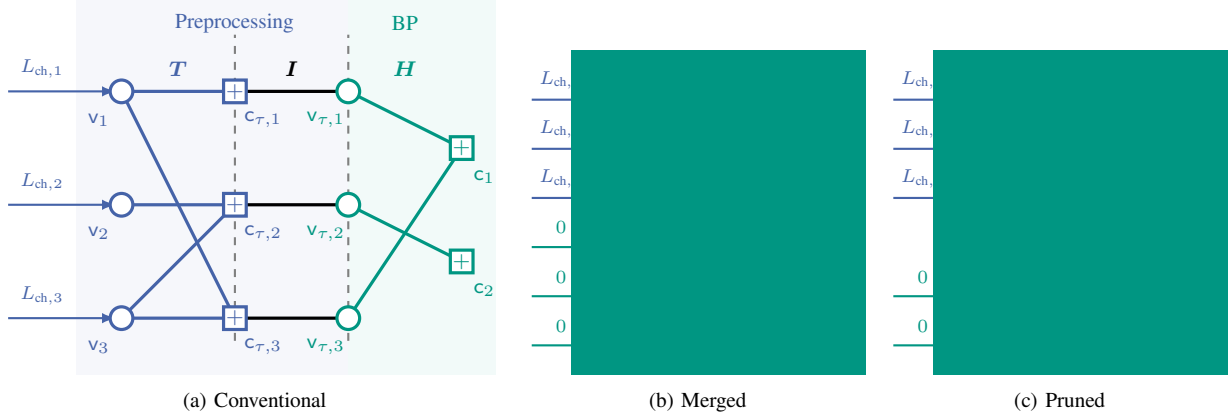


Fig. 2. Graphical illustration of the transformation of the conventional path from GAED in (a) via the merged Tanner graph in (b) to the pruned Tanner graph in (c).

the ensemble's performance. Thus, GAED is a promising candidate to enhance decoding performance, particularly for short block length codes. However, open questions remain. First, each path performs its respective preprocessing once and then ignores the additional knowledge about the code structure provided by the automorphism. Second, the decoder in each path has no access to the originally received LLR vector \mathbf{L} but only to the preprocessed values \mathbf{L}_{τ_ℓ} . Thus, in the following section, we propose an alternative perspective aiming to avoid explicit preprocessing by merging it with BP decoding and, thus, iteratively and jointly exploiting the knowledge of the automorphism and the unprocessed LLR vector during decoding. Hence, we expect an improved performance of the ensemble by avoiding information loss in the preprocessing of the respective paths.

III. IMPROVED GENERALIZED AUTOMORPHISM BELIEF PROPAGATION DECODING

In this section, we improve the individual paths of GAED by avoiding explicit preprocessing as described in (2) and implicitly performing the according mapping within BP of a suitably extended Tanner graph.

A. Preprocessing as Extended Tanner Graph

To this end, we realize the preprocessing as part of a larger Tanner graph consisting of $2n$ VNs forming the set \mathfrak{V}' and $n + m$ CNs forming the set \mathfrak{C}' , respectively. The extended Tanner graph simultaneously represents the structure of the PCM of the code and describes the effects of the preprocessing due to generalized automorphism \mathbf{T} . Figure 2 illustrates the transformation process of the graph.

As illustrated in Fig. 2(a), the extended Tanner graph is defined to consist of $2n$ VNs $\mathfrak{V}' = \mathfrak{V} \cup \mathfrak{V}_\tau$ with $\mathfrak{V} := \{v_i : i = 1, \dots, n\}$ and $\mathfrak{V}_\tau := \{v_{\tau,i} : i = 1, \dots, n\}$. Herein, v_i is denoting the i th code bit of the estimated transmitted codeword and $v_{\tau,i}$ is denoting the i th position of the estimated preprocessed codeword after applying the generalized automorphism \mathbf{T} , respectively.

The set of check nodes \mathfrak{C}' of the extended Tanner graph is defined by $\mathfrak{C}' = \mathfrak{C} \cup \mathfrak{C}_\tau$ with \mathfrak{C} denoting the original check

nodes, described by PCM \mathbf{H} , and \mathfrak{C}_τ denoting additional check nodes representing the preprocessing. Note that, according to (2), each row operation of the generalized automorphism \mathbf{T} can be interpreted as a CN, in total yielding n additional CNs that form the set \mathfrak{C}_τ .

In order to consider the fact that v_i is contributing to the j th preprocessed value $v_{\tau,j} = (\mathbf{T}\mathbf{v})_j$, the following connections are constituted:

- VN $v_i \in \mathfrak{V}$ is connected to (new) CN $c_{\tau,j}$ if and only if $T_{j,i} \neq 0$, i.e., if v_i is participating in $v_{\tau,j}$
- CN $c_{\tau,j}$ is connected to (new) VN $v_{\tau,j} \in \mathfrak{V}_\tau$ and not connected to any other $v_{\tau,\ell} \in \mathfrak{V}_\tau, \ell \neq j$

Therefore, the Tanner graph associated with the preprocessing, connecting \mathfrak{V} and \mathfrak{V}_τ by CNs \mathfrak{C}_τ , is considered as the Tanner graph of the PCM

$$\mathbf{H}_{\text{pp}} = (\mathbf{T} \quad \mathbf{I}_{n \times n}) \in \mathbb{F}_2^{n \times 2n}.$$

of a low-density generator-matrix (LDGM) code. Now, the GAED preprocessing step is realized by a message passing of the channel information from the VNs \mathfrak{V} in a check node update in \mathfrak{C}_τ and a VN update in VNs \mathfrak{V}_τ .

Next, in GAED, as illustrated in the right-hand side of Fig. 2(a), BP decoding is performed on the Tanner graph associated with the original PCM \mathbf{H} using the preprocessed values in \mathfrak{V}_τ and the CNs in \mathfrak{C} . In Fig. 2(a), the unprocessed channel information is unavailable during BP decoding.

We propose to transform the graph into the structure depicted in Fig. 2(b). Therein, we stack the n VNs in \mathfrak{V} below the n VNs in \mathfrak{V}_τ and the m CNs in \mathfrak{C}_τ above the n CNs in \mathfrak{C} , respectively, while maintaining the edges. This yields a larger Tanner graph, consisting of $2n$ VNs \mathfrak{V}' and $n + m$ CNs \mathfrak{C}' , associated with a PCM

$$\mathbf{H}_{\text{IGAED}} = \begin{pmatrix} \mathbf{T} & \mathbf{I}_{n \times n} \\ \mathbf{0}_{m \times n} & \mathbf{H} \end{pmatrix} \in \mathbb{F}_2^{(n+m) \times 2n}. \quad (3)$$

Hereby, the first n VNs are connected to the LLR vector \mathbf{L} , i.e., to \mathfrak{V} and possess unprocessed channel information. The remaining n VNs account for the auxiliary checks in \mathfrak{V}_τ , representing the preprocessing. No a-priori information is known about the VNs in \mathfrak{V}_τ which, therefore, are considered

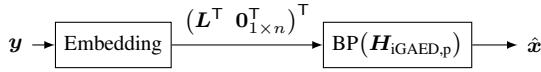


Fig. 3. A path of iGAED using the pruned matrix $\mathbf{H}_{\text{iGAED},p}$. The embedding maps the channel output to an extended LLR vector of dimension $2n$ by appending zeros.

as erased.² Note that the merging process can also be interpreted as a different decoding schedule based on the graph depicted in Fig. 2(a) where all VNs and CNs are updated in parallel, respectively.

B. Pruning of the Extended Tanner Graph

To simplify the structure of the Tanner graph, note that a transformation matrix \mathbf{T} with weight over permutation $\Delta(\mathbf{T}) < n$ possesses at least one row with a single non-zero entry, resulting in a CN $c_{\tau,j}$ of degree 2 in the Tanner graph defined by \mathbf{H}_{pp} . Assume that $c_{\tau,j}$ is connected to $v_i \in \mathfrak{V}$ and $v_{\tau,\ell} \in \mathfrak{V}_{\tau}$. Then, similar to [14], the extended Tanner graph can be simplified by merging the VN $v_{\tau,\ell} \in \mathfrak{V}_{\tau}$ into the VN $v_i \in \mathfrak{V}$, rerouting all other connections of $v_{\tau,\ell}$ to v_i . Note that a VN after merging corresponds to both a code bit of the received codeword \mathbf{y} as well as a bit within the preprocessed codeword \mathbf{y}_{τ} . Furthermore, note that the adaptation of $\mathbf{H}_{\text{iGAED}}$ can be realized by column additions and row/column deletions. The PCM after pruning is denoted by $\mathbf{H}_{\text{iGAED},p}$.

A single path of iGAED is depicted in Fig. 3. Thereby, the channel output is mapped to its LLR, extended to length $2n$ as described beforehand, and BP decoding is performed using the Tanner graph associated with $\mathbf{H}_{\text{iGAED}}$ or its pruned version $\mathbf{H}_{\text{iGAED},p}$, where the VNs associated with an actual code bit possess channel information and the others are initialized by zero LLRs.

Note that iGAED involves a higher number of CNs and VNs, resulting in a slight increase in complexity compared to GAED.

Example: The transformation matrix³ and the PCM of Fig. 2 are given by

$$\mathbf{T} = \begin{pmatrix} 1 & 0 & 0 \\ 0 & 1 & 1 \\ 1 & 0 & 1 \end{pmatrix}, \quad \mathbf{H} = \begin{pmatrix} 1 & 0 & 1 \\ 0 & 1 & 0 \end{pmatrix},$$

respectively, resulting in

$$\mathbf{H}_{\text{iGAED}} = \begin{pmatrix} 1 & 0 & 0 & 1 & 0 & 0 \\ 0 & 1 & 1 & 0 & 1 & 0 \\ 1 & 0 & 1 & 0 & 0 & 1 \\ 0 & 0 & 0 & 1 & 0 & 1 \\ 0 & 0 & 0 & 0 & 1 & 0 \end{pmatrix}.$$

CN $c_{\tau,1}$ has only two neighbors $v_1 \in \mathfrak{V}$ and $v_{\tau,1} \in \mathfrak{V}_{\tau}$. Thus, VNs v_1 and $v_{\tau,1}$ can merged into VN $v_1 \in \mathfrak{V}$, see Fig. 2(c). Edge $(v_{\tau,1}, c_1)$ is rerouted as (v_1, c_1) .

²Another possibility is to use the preprocessing from GAED to obtain information about the VNs from \mathfrak{V}_{τ} . However, our simulation results showed equal performances with respect to error rates for both setups. Hence, we erase the additional bits to avoid the explicit calculation of the preprocessing step.

³Note that the transformation \mathbf{T} used in this example and in Fig. 2 does not constitute an actual automorphism, but is chosen for simplicity of illustration.

TABLE I
CODE PARAMETERS [10]

Code	\mathcal{C}_2	$\mathcal{C}_{\text{CCSDS}}$	\mathcal{C}_3	\mathcal{C}_{BCH}
n	32	32	63	63
k	16	16	45	45
d_{\min}	5	4	5	7
$\Delta(\mathbf{T})$	10	—	5	—
$\Delta(\mathbf{T}^{-1})$	13	—	6	—
$\Delta(\mathbf{T}^2)$	19	—	11	—
$\Delta((\mathbf{T}^2)^{-1})$	24	—	12	—

Merging $v_{\tau,1}$ and v_1 is achieved by adding the column associated to $v_{\tau,1}$ onto the column associated to v_1 and deleting the row associated to $c_{\tau,1}$ yielding the pruned matrix

$$\mathbf{H}_{\text{iGAED},p} = \begin{pmatrix} 0 & 1 & 1 & 1 & 0 \\ 1 & 0 & 1 & 0 & 1 \\ 1 & 0 & 0 & 0 & 1 \\ 0 & 0 & 0 & 1 & 0 \end{pmatrix}.$$

IV. RESULTS

To demonstrate the validity of our approach, we consider two codes $\mathcal{C}_2(32, 16)$ and $\mathcal{C}_3(63, 45)$ from [10] with weight over permutation $\Delta(\mathbf{T}) = 10$ and $\Delta(\mathbf{T}) = 5$, respectively. In [10], codes with associated automorphisms are designed based on the Frobenius normal form. For comparison, we include two reference codes, namely $\mathcal{C}_{\text{CCSDS}}(32, 16)$ from [15] and the Bose–Chaudhuri–Hocquenghem (BCH) code $\mathcal{C}_{\text{BCH}}(63, 45)$. We analyze the frame error rate (FER) of different decoding algorithms by performing Monte-Carlo simulations. All BP decodings use normalized min-sum decoding with normalization factor $\frac{3}{4}$ and flooding schedule [16].⁴

When designing automorphisms, we exploit that the automorphism group is closed under multiplication and inversion of elements. Thus, given \mathbf{T} , we obtain additional automorphisms \mathbf{T}^{-1} , \mathbf{T}^2 , and $(\mathbf{T}^2)^{-1}$ using basic \mathbb{F}_2 matrix operations. The code parameters and the weights over permutation of the generalized automorphisms are collected in Table I. The minimum Hamming distances and approximate performance of ML decoding of \mathcal{C}_2 , \mathcal{C}_3 , and \mathcal{C}_{BCH} are taken from [10], whereas the minimum Hamming distance of $\mathcal{C}_{\text{CCSDS}}$ is calculated using the algorithm proposed in [17] and the performance of ML decoding stems from [15].

Similar to the notation used in [10], BP- p denotes BP decoding using p iterations and GAED- K -BP- p refers to GAED consisting of K paths comprising BP decoding with p iterations each. Following this convention, iGAED- K -BP- p corresponds to BP decoding performing p iterations on K merged and pruned graphs associated with $\mathbf{H}_{\text{iGAED},p}$ as depicted in Fig. 3. Sparse PCMs for the codes \mathcal{C}_2 , \mathcal{C}_3 , and \mathcal{C}_{BCH} are obtained using the algorithm proposed in [18]. They are used for BP decoding in GAED and as input for the merging and pruning process.

All GAED and iGAED use the identity mapping $\mathbf{T}_1 = \mathbf{I}$ in Path-1, corresponding to plain BP that typically possesses

⁴Note that sum-product algorithm yields almost identical performances.

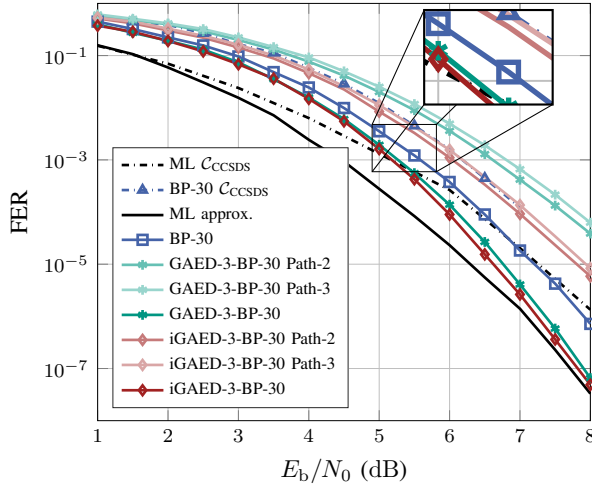


Fig. 4. Performance of different decoders for code $C_2(32, 16)$ from [10]. Additionally, the stand-alone performance of the auxiliary paths of GAED-3-BP-30 and iGAED-3-BP-30 are depicted, respectively.

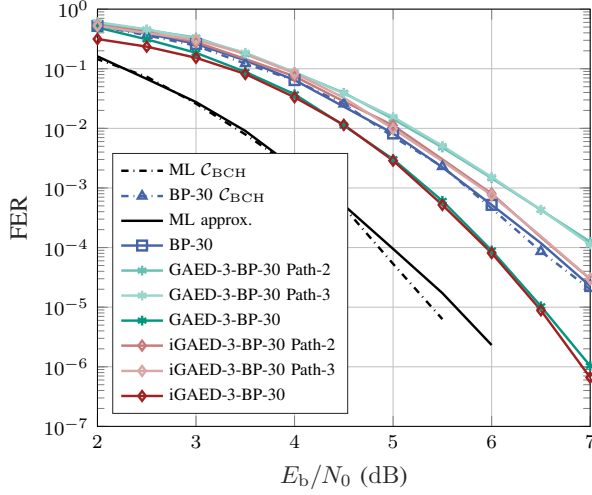


Fig. 5. Performance of different decoders for code $C_3(63, 45)$ from [10]. Additionally, the stand-alone performance of the auxiliary paths of GAED-3-BP-30 and iGAED-3-BP-30 are depicted, respectively.

the best performance among all individual paths. To express this fact, the supplementary paths are termed auxiliary paths from now on. GAED-3-BP- p and iGAED-3-BP- p additionally employ $T_2 = T$ and $T_3 = T^{-1}$ in their auxiliary paths, whereas GAED-5-BP- p as well as iGAED-5-BP- p additionally use paths relying on $T_4 = T^2$ and $T_5 = (T^2)^{-1}$. To address different use cases of a possible 6G standard, we consider a *reliable* scenario operating at a target FER of 10^{-3} and an *ultra-reliable* scenario operating at a target FER of 10^{-5} .

Figure 4 and Fig. 5 illustrate the FER over E_b/N_0 of GAED-3-BP-30 and iGAED-3-BP-30 for the codes C_2 and C_3 compared to the performances of their respective constituent paths. Additionally, we depict the ML performance of the codes as well as the ML and BP-30 performance of the respective reference codes.

For both codes, GAED-3-BP-30 and iGAED-3-BP-30 significantly improve decoding performance compared to stand-alone BP-30. For code C_2 , we observe a gain of 0.45 dB

and 0.5 dB at an FER of 10^{-3} which increases to 0.5 dB and 0.6 dB at an FER of 10^{-5} , respectively. Therefore, the proposed iGAED-3-BP-30 yields an additional gain of 0.05 dB and 0.1 dB compared to conventional GAED-3-BP-30 in the reliable and ultra-reliable scenario, respectively.

Note that the designed automorphism T of code C_2 as well as its inverse T^{-1} possess a relatively high weight over permutation in the order of $n/3$, resulting in a notable information loss during preprocessing. Consequently, at an FER of 10^{-3} , GAED-3-BP-30 Path-2 and Path-3 require an additional SNR of 1 dB and 1.1 dB compared to BP-30, respectively. Considering iGAED-3-BP-30 Path-2 and Path-3, the SNR gap of the auxiliary paths to BP-30 is reduced to 0.5 dB and 0.6 dB, respectively. Hence, the improvement of iGAED-3-BP-30 compared to GAED-3-BP-30 can be attributed to the significantly better performance of the auxiliary paths. Furthermore, it is interesting to highlight that the performance of iGAED-3-BP-30 almost fully closes the gap to the ML performance in the high SNR regime.

For code C_3 , GAED-3-BP-30 and iGAED-3-BP-30 show a similar gain of 0.5 dB compared to BP-30 at an FER of 10^{-3} increasing to 0.6 dB at an FER of 10^{-5} . Due to the relatively low weight over permutation in the order of $n/10$ of the employed automorphisms, the SNR degradation of the auxiliary paths of GAED-3-BP-30 only amounts to 0.4 dB, significantly lower than for C_2 . Still, the proposed path structure improves the performance of the auxiliary paths yielding a respective gain of 0.2 dB at an FER of 10^{-3} for both iGAED-Path-2 and iGAED-Path-3 compared to GAED-Path-2 and GAED-Path-3. However, as depicted in Fig. 5, due to the relatively small weight over permutation, iGAED-3-BP-30 does not yield a clear gain in terms of error rate compared to GAED-3-BP-30 for both target FERs. Yet, it can be observed that iGAED-3-BP-30 yields an equal performance up to an E_b/N_0 of 5.5 dB and possesses better performance than GAED-3-BP-30 for higher SNR.

Next, to demonstrate the flexibility of ensemble decoding schemes such as GAED and iGAED, we increase the number of parallel paths, i.e., we increase the complexity while maintaining the latency. Additionally, we compare ensemble decoding at reduced latency to BP decoding with approximately equal complexity.

To this end, Fig. 6 depicts the FER over E_b/N_0 of GAED-5-BP-30 and iGAED-5-BP-30 comparing them to GAED-3-BP-30 and iGAED-3-BP-30 when decoding C_2 . GAED-5-BP-30 yields the lowest FER over the full whole simulated SNR regime. At a constant latency, in the ultra-reliable scenario GAED-5-BP-30 yields a gain of 0.05 dB, 0.1 dB, and 0.15 dB compared to iGAED-3-BP-30, GAED-5-BP-30 and GAED-3-BP-30, respectively. Thereby, it is interesting to highlight that iGAED-3-BP-30 outperforms GAED-5-BP-30 at both target FERs. Therefore, at a constant maximum latency, ensemble decoding schemes can provide the possibility to trade off complexity vs. performance.

Furthermore, due to the very short block length of the considered codes and the usage of normalized min-sum decoding,

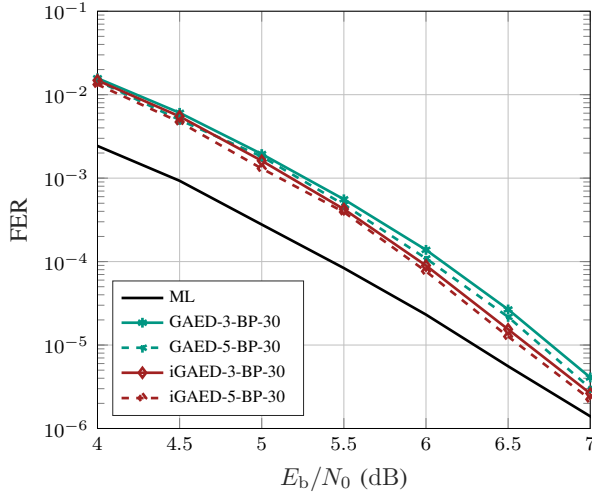


Fig. 6. Performance of GAED- K -BP-30 and iGAED- K -BP-30 for code $C_2(32, 16)$ from [10] for 3 and 5 parallel paths, respectively.

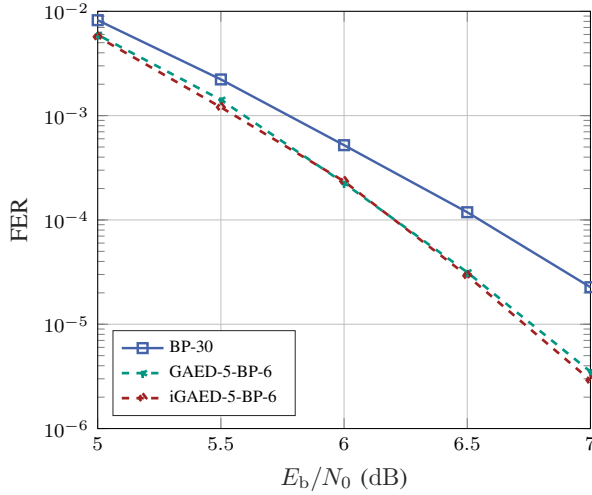


Fig. 7. Performance of GAED-5-BP-6 and iGAED-5-BP-6 for code $C_3(63, 45)$ from [10] in comparison to BP-30, i.e., at comparable complexity.

their application in a potential ultra-low latency application of 6G is inherent. To further elaborate this use case, we consider parallel decoding using only 6 iterations of min-sum decoding to reduce the decoding latency. Figure 7 depicts the FER over E_b/N_0 of GAED-5-BP-6 and iGAED-5-BP-6 in comparison to BP-30, such that the ensemble decoding schemes have five times lower latency but equal complexity when compared to the stand-alone BP decoding. Thus, two observations are noticeable. First, in particular at the target FERs, iGAED-5-BP-6 tends to yield a slightly lower FER than GAED-5-BP-6. Second, at a constant complexity and reduced latency, iGAED-5-BP-6 and GAED-5-BP-6 significantly outperform BP-30. At an FER of 10^{-3} , iGAED-5-BP-6 yields a gain of 0.3 dB compared to BP-30.

V. CONCLUSION

In this work, we showed that the preprocessing of GAED can be merged with the Tanner graph associated with BP decoding, yielding an extended Tanner graph which is then

used for decoding. This extended graph inherently combines knowledge on the preprocessing by the generalized automorphism with the BP decoding steps. Simulations have shown that iGAED can improve decoding performance compared to GAED, the benefit depending on the weight over permutation. Additionally, we demonstrated that iGAED yields significant improvement compared to BP decoding in different use-cases incorporating an URLLC scenario. Moreover, we observed possible close-to-ML performance of iGAED in the high SNR regime, showing that a purely BP-based scheme can close the gap to ML decoding in a short block length regime, depending on the code structure. An interesting open question for future works is the analysis of different decoding schedules on the pruned Tanner graph.

REFERENCES

- [1] W. Saad, M. Bennis, and M. Chen, "A vision of 6G wireless systems: Applications, trends, technologies, and open research problems," *IEEE Netw.*, vol. 34, no. 3, pp. 134–142, May/June 2020.
- [2] M. Geiselhart, F. Krieg, J. Clausius, D. Tandler, and S. ten Brink, "6G: A welcome chance to unify channel coding?" *IEEE BITS the Information Theory Magazine*, pp. 1–12, 2023.
- [3] C. Kestel, M. Geiselhart, L. Johannsen, S. ten Brink, and N. Wehn, "Automorphism ensemble polar code decoders for 6G URLLC," in *Proc. Int. ITG Workshop on Smart Antennas and Conf. on Systems, Commun., and Coding (WSA & SCC)*, Braunschweig, Germany, Mar. 2023.
- [4] R. G. Gallager, "Low density parity check codes," Ph.D. dissertation, Mass. Inst. Tech. (MIT), Cambridge, 1960.
- [5] T. Richardson and R. Urbanke, *Modern Coding Theory*. Cambridge University Press, 2008.
- [6] T. Hehn, J. B. Huber, S. Laendner, and O. Milenkovic, "Multiple-bases belief-propagation for decoding of short block codes," in *Proc. IEEE Int. Symp. Inf. Theory (ISIT)*, Nice, France, Jun. 2007.
- [7] T. Hehn, J. B. Huber, P. He, and S. Laendner, "Multiple-bases belief-propagation with leaking for decoding of moderate-length block codes," in *Proc. Int. ITG Conf. on Source and Channel Coding (SCC)*, Ulm, Germany, Jan. 2008.
- [8] M. Geiselhart, A. Elkelesh, M. Ebada, S. Cammerer, and S. ten Brink, "Automorphism ensemble decoding of Reed-Muller codes," *IEEE Trans. Commun.*, vol. 69, no. 10, pp. 6424–6438, Oct. 2021.
- [9] M. Geiselhart, M. Ebada, A. Elkelesh, J. Clausius, and S. ten Brink, "Automorphism ensemble decoding of quasi-cyclic LDPC codes by breaking graph symmetries," *IEEE Commun. Lett.*, vol. 26, no. 8, pp. 1705–1709, Aug. 2022.
- [10] J. Mandelbaum, H. Jäkel, and L. Schmalen, "Generalized automorphisms of channel codes: Properties, code design, and a decoder," in *Proc. Int. Symp. on Topics in Coding (ISTC)*, Brest, France, Sept. 2023.
- [11] J. Mandelbaum, S. Miao, H. Jäkel, and L. Schmalen, "Endomorphisms of linear block codes," *arXiv preprint arXiv:2402.00562*, 2024.
- [12] F. J. MacWilliams and N. J. A. Sloane, *The Theory of Error Correcting Codes*, ser. North-Holland Mathematical Library. Elsevier, 1977.
- [13] J. Hagenauer, E. Offer, and L. Papke, "Iterative decoding of binary block and convolutional codes," *IEEE Trans. Inf. Theory*, vol. 42, no. 2, pp. 429–445, Mar. 1996.
- [14] S. Cammerer, M. Ebada, A. Elkelesh, and S. ten Brink, "Sparse graphs for belief propagation decoding of polar codes," in *Proc. IEEE Int. Symp. Inf. Theory (ISIT)*, Vail, CO, USA, Jun. 2018.
- [15] M. Helmling, S. Scholl, F. Gensheimer, T. Dietz, K. Kraft, S. Ruzika, and N. Wehn, "Database of Channel Codes and ML Simulation Results," www.uni-kl.de/channel-codes, 2019, accessed 2023-01-04.
- [16] F. Angarita, J. Valls, V. Almenar, and V. Torres, "Reduced-complexity min-sum algorithm for decoding LDPC codes with low error-floor," *IEEE Trans. Circuits Syst.*, vol. 61, no. 7, pp. 2150–2158, Feb. 2014.
- [17] M. Puneekar, F. Kienle, N. Wehn, A. Tanatmis, S. Ruzika, and H. W. Hamacher, "Calculating the minimum distance of linear block codes via integer programming," in *Proc. Int. Symp. on Turbo Codes & Iterative Inf. Process. (ISTC)*, Brest, France, Sept. 2010.
- [18] F. Gensheimer, T. Dietz, S. Ruzika, K. Kraft, and N. Wehn, "Improved maximum-likelihood decoding using sparse parity-check matrices," in *Proc. Int. Conf. on Telecommun. (ICT)*, Saint Malo, France, Jun. 2018.